P3.5 FUTURE CHANGE IN NORTHERN HEMISPHERE WINTERTIME ATMOSPHERIC BLOCKING SIMULATED BY A 20-KM MESH ATMOSPHERIC GLOBAL CIRCULATION MODEL

Mio MATSUEDA[1,2] *, Ryo MIZUTA[1,2], and Shoji KUSUNOKI[2]
1: Advanced Earth Science and Technology Organization, Tsukuba, Japan
2: Meteorological Research Institute, Tsukuba, Japan

1. INTRODUCTION

Atmospheric blocking sometimes persists for a long time, leading to extremely high or low temperature and severe precipitation anomalies over the surrounding area. In February 1989, a blocking remained over Alaska for approximately one month (Tanaka and Milkovich 1990). The monthly mean temperature at Barrow was 18°C warmer than normal. The anomaly corresponded to 4 climatological standard deviations, whereas a number of new record-low temperatures on the surface were reported in interior Alaska at the end of January. In February 1998, heavy precipitation related to coastal blocking occurred over the Southern California (Neiman et al. 2004). The daily precipitation at Los Angeles was equivalent to climatological monthly precipitation. In August 2003, a heat wave caused by a very robust and persistent blocking occurred over Europe (Black et. al. 2004). More than 35,000 people died as a result of this heat wave. Agricultural products also experienced severe damage. A large number of studies dealing with extreme events related to the blocking, the mechanism of the blocking, and model performances in simulating the blocking have been conducted.

It also seems to be very important to estimate the blocking frequency in the future climate. Nevertheless, future change in the blocking was not reported in the IPCC-AR4 report (Solomon et. al. 2007). In general, it is well known that the general circulation models underestimate the blocking frequency (Plamer et. al. 2008; Pelly and Hoskins 2003; D'Andrea et al. 1998). This fact might lead to difficulty in determining the future change of the blocking with reliability.

We have developed a 20-km mesh atmospheric global circulation model (AGCM; TL959L60) for global warming projection (Mizuta et. al. 2006). In this study, we focus on the frequency and the duration of the blocking simulated by the TL959L60 model and the lower-resolution models, TL319L60 (60 km), TL159L40 (120 km), and TL95L40 (180 km), for the Northern Hemisphere winter (December – February) in the present-day (1979–2003) and the future (2075–2099) climates. Also, in order to estimate uncertainty in the future projection of the blocking, SST and initial value ensemble simulations were conducted using a 60-km mesh AGCM.

* *Corresponding author address:* Mio Matsueda, MRI, Climate Research Department, 1-1 Nagamine, Tsukuba, Ibaraki, Japan, 305-0052; e-mail: mimatsue@mri-jma.go.jp

2. MODEL AND METHOD

2.1 *Model*

The AGCM used in this study is a climate model for long-term climate simulation of Meteorological Research Institute (MRI). This model is based on the operational global model for medium-range numerical weather prediction at Japan Meteorologocal Agency (JMA). The details of the AGCM are described in Mizuta et al. (2006). The simulations were performed at a triangular truncation 959 with linear Gaussian grid (TL959) in the horizontal and 60 vartical levels. The horizontal resolution corresponds to a grid size of about 20 km. The AGCMs with the lower-horizontal resolutions, TL319L60 (60 km), TL159L40 (120 km), and TL95L40 (180 km), were also used in order to evaluate impact of the horizontal resolution on the blocking simulation. It is noted that the vertical resolution of the TL959 and the TL319 models is different from that of the TL159 and the TL95 models. The model integrations were conducted for the present-day (1979–2003) and the future (2075–2099) climates.

2.2 *Boundary Condition*

For the present-day simulation, the AGCM was integrated with observed historical SST (HadISST). For the future simulation, we prescribed SST in which the change in SST projected by the CMIP3 multi-model ensemble mean is added to the HadISST (Mizuta et al. 2008). IPCC SRES A1B scenario was assumed for future emission of the green house gases.

2.3 *Ensemble simulations*

In order to estimate uncertainty in the future projection of the blocking, the SST and initial value ensemble simulations were conducted using a 60-km mesh AGCM. For the present-day simulation, the initial value ensemble simulations were conducted with three arbitrary initial values. For the future simulation, the SST and initial value ensemble simulations were conducted with four SSTs and three arbitrary initial values (ensemble size is 12). The four SSTs were made by the addition of the change in SST projected by the CMIP3 multi-model ensemble mean, the CSIRO_Mk3.0, the MRI-CGCM2.3.2, and the MIROC3.2 (hires) to the HadISST. It is noted that the MIROC3.2 (hires) (CSIRO_Mk3.0) model shows a high (low) climate sensitivity.

2.4 *Blocking Index*

The data used in this study consists of daily 500 hPa geopotential height field at 12 Z, both observed and produced by long integration of the AGCM. The reanalysis by the JMA (JRA25; Onogi et al. 2007) was adopted as the observation data for the period December 1979 – February 2004. Before the calculation of the blocking index, the data was interpotated into 1.25 degree grid spacing.

An objective blocking index, based on D'Andrea et al. (1998), was used in this study. The following definition is essentially derived from the work of Lejenãs and Økland (1983). Here only a brief definition is given. The 500 hPa geopotential height meridional gradients, GHGS and GHGN, are computed for each latitude:

$$\begin{cases} \text{GHGS} &= \dfrac{Z(\phi_0) - Z(\phi_s)}{\phi_0 - \phi_s}, \\ \text{GHGN} &= \dfrac{Z(\phi_n) - Z(\phi_0)}{\phi_n - \phi_0}, \end{cases} \tag{1}$$

where:

$$\begin{cases} \phi_n &= 77.5^\circ\text{N} \pm \Delta, \\ \phi_0 &= 60.0^\circ\text{N} \pm \Delta, \\ \phi_s &= 40.0^\circ\text{N} \pm \Delta, \end{cases}$$

$$\Delta = 0^\circ,\ 1.25^\circ,\ 2.5^\circ,\ 3.75^\circ,\ 5.0^\circ.$$

A specific longitude on a specific day is defined as blocked if both following conditions are satisfied (for at least one value of Δ):

$$\begin{cases} \text{GHGS} > 0, \\ \text{GHGN} < -5\text{m/deg lat.} \end{cases} \tag{2}$$

Similarly to D'Andrea et al. (1998), the two main sectors of the Northern Hemisphere that are particularly prone to blocking are defined, with the following longitudinal limits:

$$\begin{aligned} \text{Euro-Atlantic} &: 26.25^\circ\text{W} - 41.25^\circ\text{E} \\ \text{Pacific} &: 120^\circ\text{E} - 140^\circ\text{W} \end{aligned}$$

A sector is then defined to be blocked if three or more adjacent longitudes within its limits are blocked according to the previous local and instantaneous index definition ("sector blocking"). The blocking duration is calculated for the sector blocking, and the loose time-continuity constraint is introduced as follows:

> When two successive days are considered blocked by the index in a sector and are followed by a non-blocked day and then by two more successive blocked days, the whole event is considered as a five day long block, assuming the "hole" simply as an index failure. An analogous "tapering" criterion is applied in the cases of a single non-blocked day preceded (followed) by three blocked days and followed (preceded) by a single blocked day.

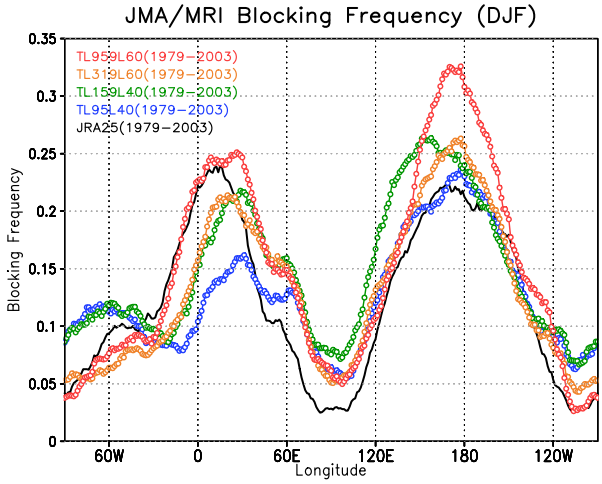

FIG. 1: Northern Hemisphere wintertime blocking frequency as function of longitude for the JMA/MRI models with 4 different horizontal resolutions: TL959L60 (20km; red), TL319L60 (60 km; orange), TL159L40 (120 km; green), and TL95L40 (180 km; blue), and the JRA25 (1979–2003; black) in the present-day climate (1979-2003).

3. RESULTS

3.1 *Present-Day Climate Experiments*

Figure 1 illustrates the blocking frequency as function of longitude for the JRA25 and the AGCMs in the present-day climate. In the Northern Hemisphere wintertime , the observed blocking frequency (black line in each panel) shows the well-known blocking maxima in the Euro-Atlantic and the Pacific sectors. The Ural blocking, a third secondary peak, is also visible at around 60°E.

It is well known that general circulation models tend to underestimate the blocking frequency (Plamer et. al. 2008; Pelly and Hoskins 2003; D'Andrea et al. 1998). It is found that the TL959L60 shows good agreement with the JRA25 in respect to the Euro-Atlantic blocking frequency. The higher the horizontal resolution is, the better the blocking frequency is simulated. All the models, however, tends to overestimate the frequency of the Euro-Atlantic blocking occurring over the land. The TL959L60 can simulate the long-lived blocking well, while the horizontal resolution of the TL319L60 is not sufficient yet for the simulation of the long-lived blocking (not shown). The lower-resolution models are unable to resolve baroclinic eddies adequately, and as their effect seems to intervene especially in blocking maintenance processes, this lack of baroclinic eddy forcing may lead to simulate a larger number of short-lived blocking than observed. These results are consistent with that of Tibaldi et al. (1997), who indicated that an increase of the model resolution is important to improve the simulation of blocking in the Euro-

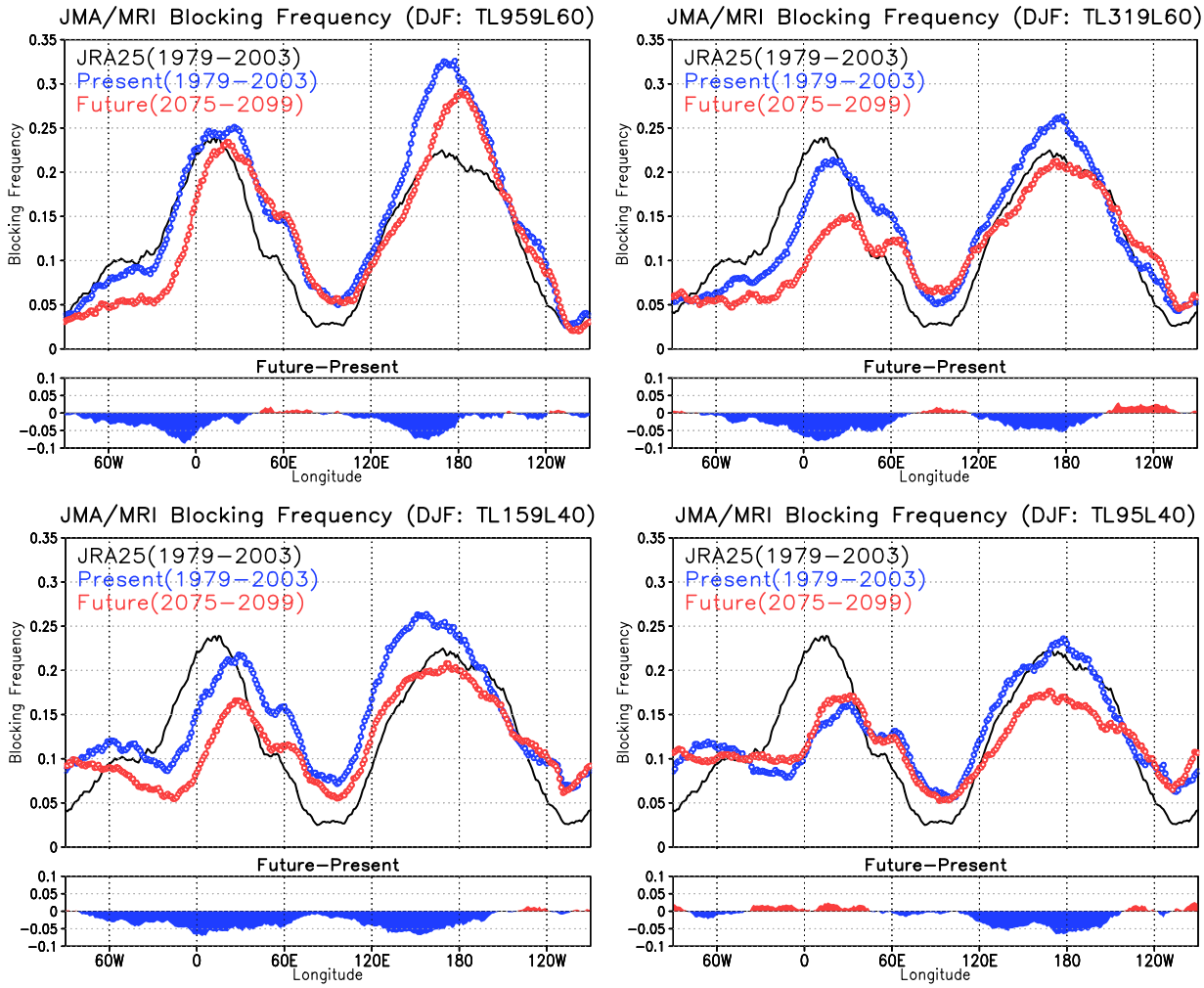

FIG. 2: Northern Hemisphere wintertime blocking frequency as function of longitude for the JMA/MRI models with 4 different horizontal resolutions: TL959L60 (20km; upper left), TL319L60 (60 km; upper right), TL159L40 (120 km; lower left), and TL95L40 (180 km; lower right). The black, blue, and red lines in the each panel are for the JRA25 (1979–2003), the present-day climate run (1979–2003), and the future climate run (2075–2099), respectively.

Atlantic sector.

On the other hand, the horizontal resolution might not be important for the simulation of the Pacific blocking. The lowest-resolution model of the TL95L40 simulates the Pacific blocking frequency well, whereas the higher-resolution models overestimate it. In particular, the TL959L60 shows the highest frequency, which is 1.5 times the observation. The TL959L60 has large bias of 500 hPa height climatology relative to the JRA25 over the North Pacific region (not shown). This might lead to the overestimation of the Pacific blocking frequency. Easily expected from the fact the TL95L40 shows the good agreement with the JRA25, the TL95L40 simulates the long-lived Pacific blocking well (not shown). It is considered that the maintenance mechanism of the Pacific blocking is different from that of the Euro-Atlantic blocking, as suggested in Tibaldi et al. (1997).

In addition, we conducted the ensemble simulations using a 60-km AGCM. The ensemble simulations were started from three arbitrary initial values. The uncertainty in the simulated blocking frequency is shown in Fig. 3 as ± 1 standard deviation of three ensemble members (blue shaded area). It is found that the uncertainty in the simulated blocking frequency is relatively small compared with the ensemble mean of the blocking frequency.

3.2 *Future Climate Experiments*

Figure 2 illustrates the future change of the blocking frequency. In the future climate, the Euro-Atlantic blocking frequency decreases, except for the TL95L40. In the TL959L60, the Euro-Atlantic blocking frequency over the land around 60°E does not change, whereas the fre-

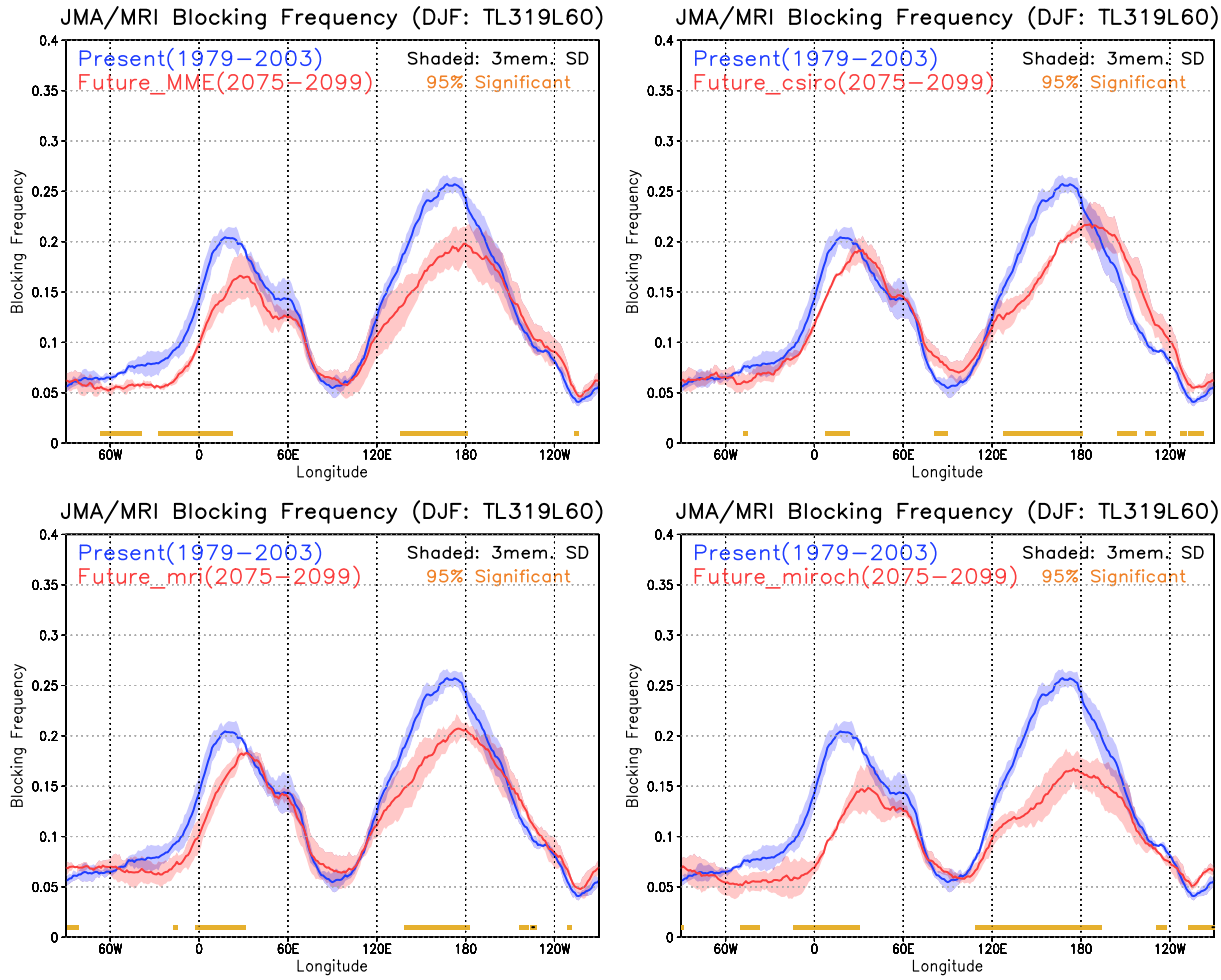

FIG. 3: Future change in Northern Hemisphere wintertime blocking frequency simulated by a 60-km mesh JMA/MRI AGCM with 4 different SSTs: CMIP3-MME SST (upper left), CSIRO_Mk3.0 SST (upper right), MRI-CGCM2.3.2 SST (lower left), and MIROC3.2 (hires) SST (lower right). The blue and red lines are for 3-member initial value ensemble means of the blcoking frequency in the present-day climate run (1979–2003) and the future climate run (2075–2099), respectively. The blue and red shaded areas show ± 1 standard deviation of the blocking frequency measured by 3 initial value ensemble members.

quency around the Greenwich meridian decreases. In the TL319L60 and TL159L40, the Euro-Atlantic blocking frequency decreases uniformly independent of the longitude. The TL95L40, showing bad agreement with the JRA25 in the present-day climate (Fig. 1), indicates small increases of the Euro-Atlantic blocking frequency.

In terms of the Pacific blocking, all the models indicate the decreases in the Pacific blocking frequency. The frequency around 150°W tends to be same as that in the present-day climate simulation.

According to the ensemble simulations using a 60-km AGCM (upper left in Fig. 3), the decreases in the Euro-Atlantic and the Pacific blocking frequencies are likely to be certain at the 0.05 level of confidence. In addition, it is found from the SST ensemble simulations (upper right, lower left, and lower right in Fig. 3) that the more the global warming proceeds, the more the Euro-Atlantic and the Pacific blocking frequencies decrease. In particular, the significant decreases tend to appear at the west of the peak of the Euro-Atlantic and the Pacific blocking frequencies. The range of the future blocking frequency simulated by ensemble members tends to be larger than the present one. This might suggest that the decadal variation of the future blocking frequency is larger than the present one.

In terms of the Euro-Atlantic blocking duration, the TL959L60, showing the good agreement with the JRA25 in the present-day climate (Fig. 1), indicates a disappearance of the long-lived (more than 25 days) blockings (Fig. 4). The TL959L60, the TL319L60, and the TL159L40 indicate a decrease in the number of the short-lived (less than 15 days) blockings. The ensemble simulations sup-

port this result (Fig. 5). However, the ensemble simulation does not indicate the apparent decreases in the number of the long-lived (more than 25 days) blockings. This might result from the fact that the TL319L60 cannot simulate long-lived blockings well in the present-day climate.

In terms of the Pacific blocking duration, the TL95L40, showing the good agreement with the JRA25 in the present-day climate (lower right in Fig. 1), indicates a disappearance of the long-lived (more than 25 days) blockings (Fig. 6). The TL319L60 shows a decrease in the number of the long-lived (more than 25 days) blockings. The TL159L40 and the TL95L40 suggest that the short-lived (less than 15 days) blockings decrease. The ensemble simulations also indicate the decreases in the number of the long-lived (more than 25 days) blcokings (Fig. 7). The decreases in the number of the short-lived (less than 15 days) blockings are not apparent.

4. CONCLUSION

In this study, the future change in the Northern Hemisphere wintertime atmospheric blocking was investigated using 20-km, 60-km, 120-km, and 180-km mesh JMA/MRI AGCMs. It was found in the present-day climate simulation that the horizontal resolution of the AGCM is important to simulate the Euro-Atlantic blocking, whereas the AGCM with the lowest hirizontal resolution shows a good agreement with the JRA25 for the Pacific blocking frequency.

In the future climate, the Euro-Atlantic and the Pacific blocking frequencies are likely to decrease. In particular, the significant decreases tend to appear at the west of the peak of the Euro-Atlantic and the Pacific blocking frequencies. It was suggested from the ensemble simulations that the more the global warming proceeds, the more the Euro-Atlantic and the Pacific blocking frequencies decrease. The number of the Euro-Atlantic blocking decreases in all durations, whereas that of the Pacific blocking decreases in especially long duration.

ACKNOWLEDGMENTS

This work is done under the framework of the ”Projection of the change in future weather extremes using super-high-resolution atmospheric models” supported by KAKUSHIN Program of MEXT. The calculations were performed on the Earth Simulator.

REFERENCES

Black, E., M. Blackburn, G. Harrison, B. Hoskins and J. Methven, 2004: Factors contributing to the summer 2003 European heatwave, *Weather*, **59**, 217–213.

D’Andrea, F., S. Tibaldi, M. Blackburn, G. Boer, M. Déqué, M. R. Dix, B. Dugas, L. Ferranti, T. Iwasaki, A. Kitoh, V. Pope, D. Randall, E. Roeckner, D. Straus, W. Stern, H. Van den Dool, D. Williamson, 1998: Northern Hemisphere atmospheric blocking as simulated by 15 atmospheric general circulation models in the period 1979-1988. *Clim. Dyn.*, **14**, 385–407.

Lejenãs, H., and H. Ø kland, 1983: Characteristic of northern hemisphere blocking as determinated from a long time series of observational data. *Tellus*, **35A**, 350–362.

Mizuta, R., K. Oouchi, H. Yoshimura, A. Noda, K. Katayama, S. Yukimoto, M. Hosaka, S. Kusunoki, H. Kawai and M. Nakagawa, 2006: 20-km-mesh global climate simulations using JMA-GSM model – mean climate states –. *J. Meteor. Soc. Japan*, **84**, 165–185.

Mizuta, R., Y. Adachi, S. Yukimoto, and S. Kusunoki, 2008: Estimation of future distribution of sea surface temperature and sea ice using CMIP3 multi-model ensemble mean, *Tech. Rep. of the MRI*, **56**.

Neiman, P. J., P. O. G. Persson, F. M. Ralph, D. P. Jorgensen, A. B. White, and D. E. Kingsmill, 2004: Modification of Fronts and Precipitation by Coastal Blocking during an Intense Landfalling Winter Storm in Southern California: Observations during CALJET. *Mon. Wea. Rev.*, **132**, 242–273.

Onogi, K., J. Tsutsui, H. Koide, M. Sakamoto, S. Kobayashi, H. Hatsushika, T. Matsumoto, N. Yamazaki, H. Kamahori, K. Takahashi, S. Kadokura, K. Wada, K. Kato, R. Oyama, T. Ose, N. Mannoji and R. Taira, 2007: The JRA-25 Reanalysis. *J. Meteor. Soc. Japan*, **85**, 369–432.

Palmer, T. N., F. J. Doblas-Reyes, A. Weisheimer, and M. J. Rodwell, 2008: Toward Seamless Prediction: Calibration of Climate Change Projections Using Seasonal Forecasts. *Bull. Amer. Meteor. Soc.*, **89**, 459–470.

Pelly J. L. and B. J. Hoskins, 2003: A New Perspectiveon Blocking. *J. Atmos. Soc.*, **60**, 743–755.

Solomon, S., D. Qin, M. Manning, M. Marquis, K. Averyt, M. M. B. Tignor, H. L. R. Miller, Jr., and Z. Chen, 2007: *Climate Change 2007. The Physical Science Basis.*, Cambridge Press, 996pp.

Tibaldi, S., F. D’Andrea, E. Tosi, and E. Roeckner, 1997: Climatology of Northern Hemisphere blocking in the ECHAM model. *Clim. Dyn.*, **13**, 649–666.

Tanaka, H. L., and M. F. Milkovich, 1990: A heat budget analysis of the polar troposphere in and around alaska during the abnormal winter of 1988/89. *Mon. Wea. Rev.*, **118**, 1628–1639.

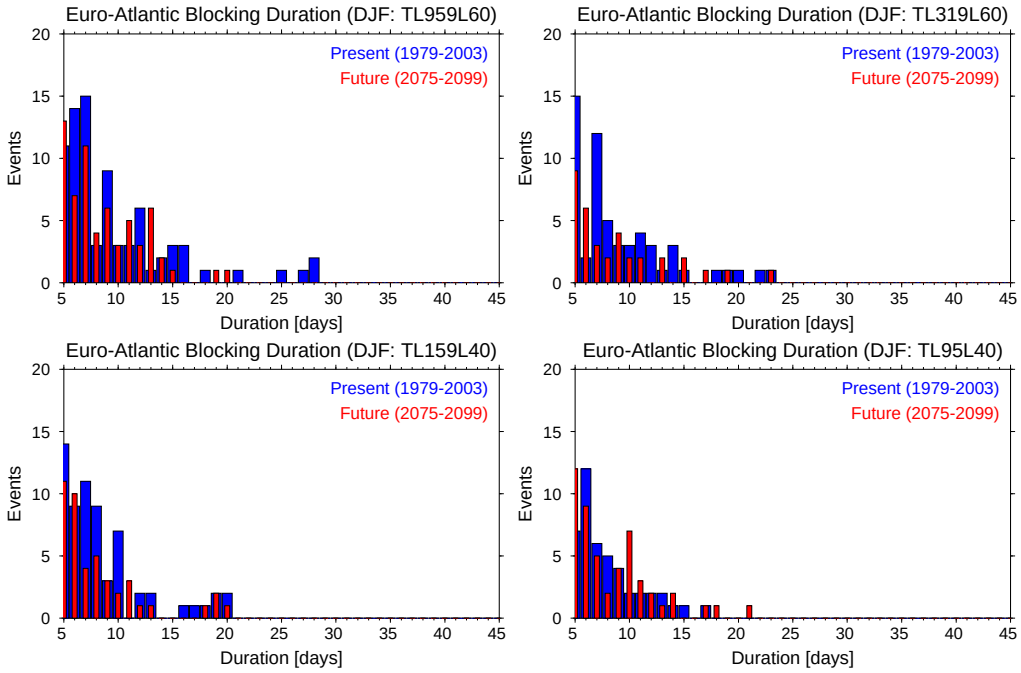

FIG. 4: Future change of wintertime Euro-Atlantic blocking duration for the JMA/MRI models with 4 different horizontal resolutions: TL959L60 (20km; upper left), TL319L60 (60 km; upper right), TL959L60 (120 km; lower left), and TL959L60 (180 km; lower right). The blue and red bars in the each panel are for the present-day climate run (1979–2003) and the future climate run (2075–2099), respectively.

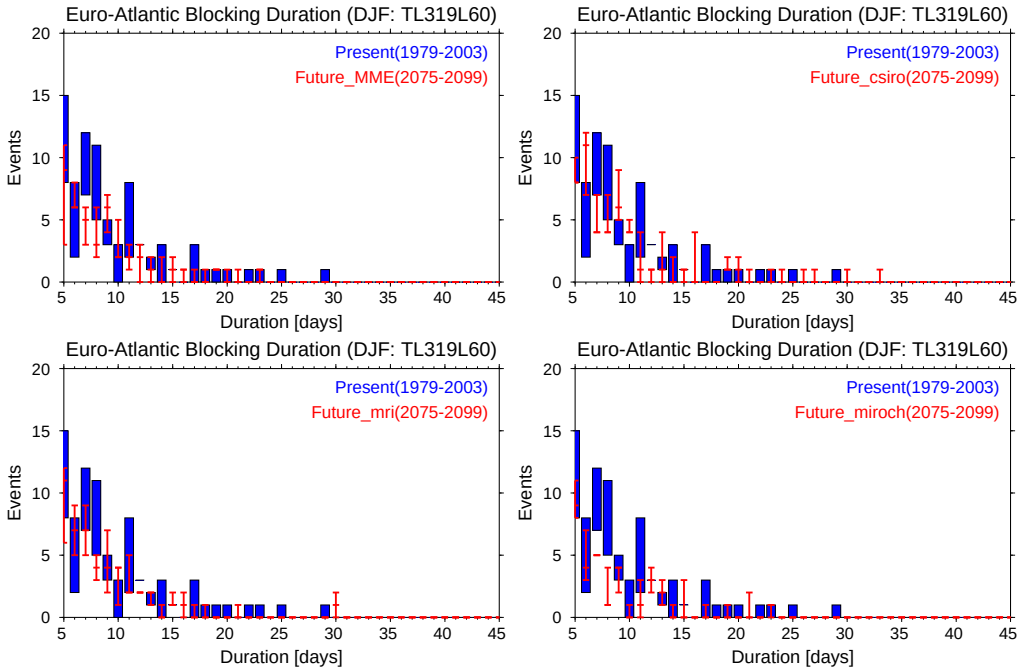

FIG. 5: Future change of wintertime Euro-Atlantic blocking duration simulated by a 60-km mesh JMA/MRI AGCM with 4 different SSTs: CMIP3-MME SST (upper left), CSIRO_Mk3.0 SST (upper right), MRI-CGCM2.3.2 SST (lower left), and MIROC3.2 (hires) SST (lower right). The blue and red bars in the each panel represent the ranges of the number of the blocking simulated by ensemble members in the present-day climate run (1979–2003) and the future climate run (2075–2099), respectively.

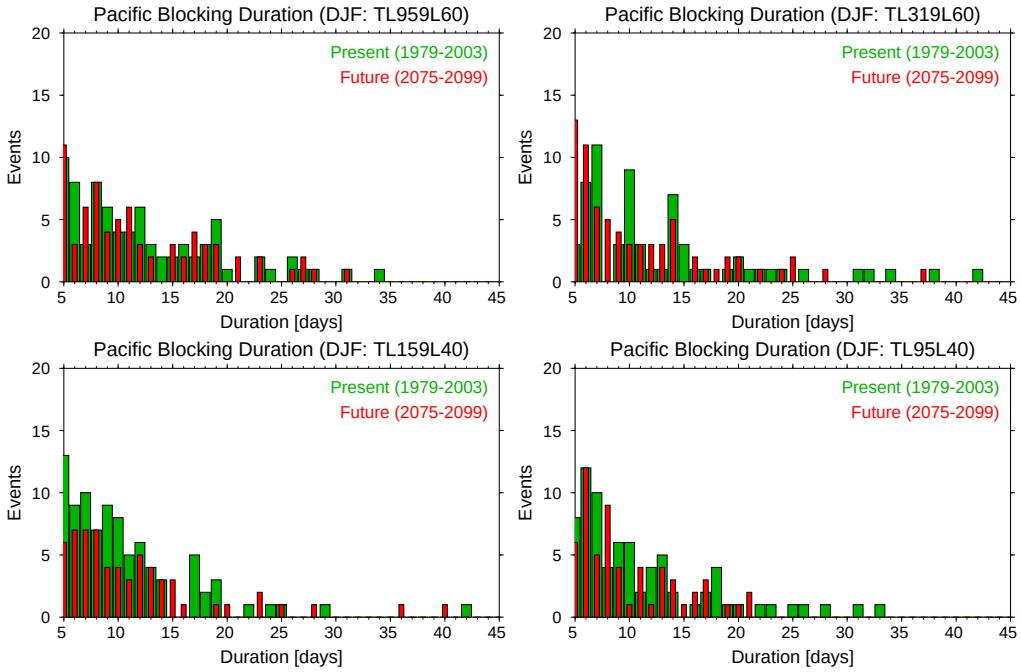

FIG. 6: Same as Fig. 4, but for the Pacific blocking.

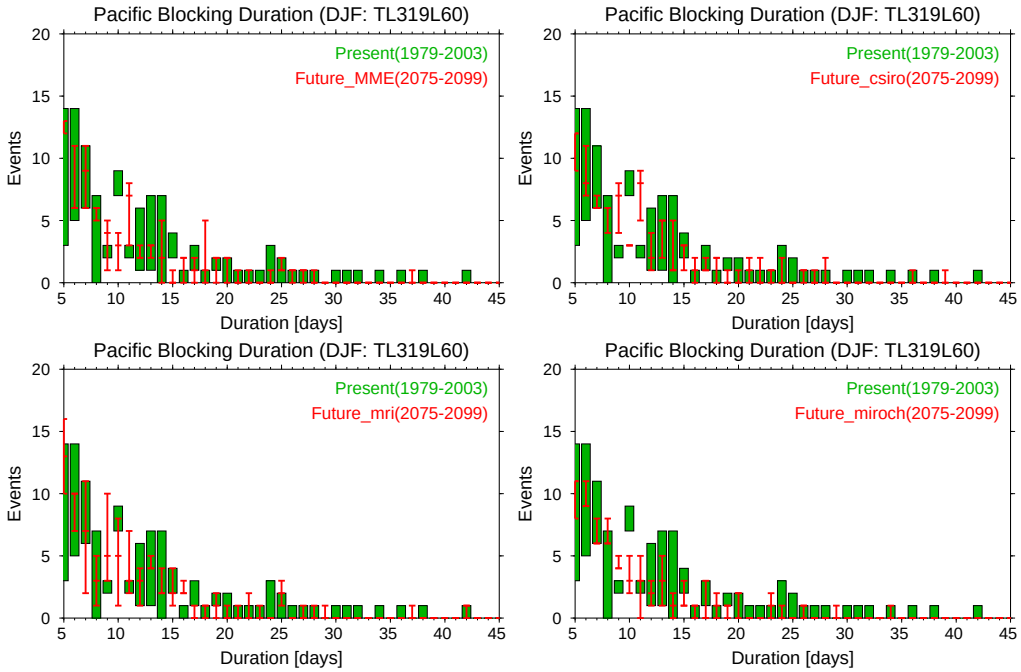

FIG. 7: Same as Fig. 5, but for the Pacific blocking.